74th International Astronautical Congress (IAC), Baku, Azerbaijan, 2-6 October 2023.

IAC-23,C1,7,4,x76458

Matryoshka Orbital Networks

J Gribben. R Clark. C Lowe. M Macdonald. *

* All, *Department of Electronic and Electrical Engineering, University of Strathclyde, Royal College Building, 204 George St, Glasgow, Scotland, G11 XW,* Joshua.Gribben@strath.ac.uk, Ruaridh.Clark@strath.ac.uk, Christopher.Lowe@strath.ac.uk, Malcolm.Macdonald102@strath.ac.uk

Abstract

This paper introduces the concept of Matryoshka Orbital Networks (MatrON), an abstraction of the orbital environment in which satellites and terrestrial targets (sources and sinks) are modelled as network nodes traversing a series of rotating, nested surfaces (shells). With Earth's surface the inner-most shell, the abstracted model is reminiscent of Matryoshka, or nesting dolls. This allows for interactions between nodes to be modelled on a surface rather than 3-D space. In this way, data can be more easily gathered on the topology of the entire MatrON network, particularly unseen opportunities for interaction between spacecraft of differing constellations. These insights enable optimising operations of new and existing constellations in the network structure which can lead to improvement of contact scheduling, mission planning, and general service delivery. Further analysis at the scale of the entire MatrON system can reveal interactions between each integrated system, thereby revealing opportunities to share benefits between interacting systems of different capability and/or operated by different stakeholders.

1. Introduction

As space becomes more accessible the congestion of Earth orbit and subsequent generation of orbital debris is a significant cause for concern in the space sector [1]. Despite this concern the number of spacecraft in orbit continues to increase exponentially. According to the United Nations Office for Outer Space Affairs (UNOOSA) more than 2,050 satellites were registered in 2022 alone, an 8.5% increase on 2021 and breaking the annual record for the 3rd consecutive year [2]. Mega-constellations make up the bulk of these registrations and this trend is expected to increase further as proposals for satellite constellations containing hundreds of thousands of satellites are submitted [3]. Starlink, an internet connectivity constellation owned by Space X, holds the record for largest satellite constellation at over 4000 satellites as of 2023 [4]. The eventual plan being to deploy 42,000 satellites in this constellation alone [5], [6].

The size of these constellations creates problems for ground-based telescopes and observatories including nonlinear crosstalk and streaks in telescope imaging [7]. However, a more catastrophic outcome of having such a densely populated orbital environment is an increasing risk of on-orbit collisions. In addition to inflicting damage to orbital equipment, it is postulated that a chain reaction of collisions could result in such a large collection of orbital debris that spaceflight would become too hazardous to conduct. This was first described by Kessler and Cour-Palais in 1978 [8] and has since become a huge cause for concern among leading space agencies [9]–[11].

Lifson et al [12] identified the drastic increase of satellites in Low Earth Orbit (LEO) and developed a new methodology for stacking orbital shells more efficiently by accounting for a higher fidelity model of Earth geopotential. The efficient use of slotting architectures is also explored by Arnas & Linares [13] who propose the use of non-self-intersecting relative orbital trajectories to analyse the orbital capacity of constellations. As research continues into the efficient management of increasingly large numbers of spacecraft, the orbital environment will become more densely packed and will require increased cooperation between stakeholders of neighbouring constellations. Lifson et al [14] suggest the LEO altitude band of 200-900km could, in time, harbour up to 1.8 million active spacecraft sustainably. A clear trend is therefore present in the literature that attempts to fill Earth's orbital environment while avoiding collisions. A new approach could empower a shift towards a more cooperative orbital space in which the resources already in place are better utilised.

As the number of satellites increases, so too will the number of space-to-ground contact opportunities. Typically, the interactions between satellites and their designated ground targets are predicted by using high-fidelity orbital propagators. These numerically calculate the position of each satellite based on their equations of motion and orbital elements from a given epoch [1]. Generally, the greater the fidelity of the propagator, the higher the computational cost. The Simplified General Perturbations (SGP4) propagator uses heavily simplified models of orbital perturbations such that the position error for propagated satellites can be high even over short timespans [15]. An improved version, SGP4-XP, was released in 2020 that increased the fidelity of the model

at the cost of a 50%-100% increase in algorithm run time [16]. Holincheck and Cathell [17] also found that this improved model provided minimal benefit in LEO propagations despite the additional fidelity. The increasingly congested nature of the orbital environment will more frequently necessitate extensive propagation and range calculations to model the interactions between spacecraft. While useful for smaller-scale propagation, the high resource requirement for these typical propagation calculations makes them impractical for the use case of modelling collections of constellations which could contain hundreds or thousands of spacecraft. This paper proposes a simplified approach that is capable of providing scalable, system-level, insights necessary to analyse the entire orbital environment.

Matryoshka Orbital Networks (MatrON) is an abstraction of the orbital environment where satellites and terrestrial targets (sources and sinks) are modelled as network nodes traversing a series of rotating, nested surfaces (shells) with the Earth's surface at the centre: reminiscent of Matryoshka (meaning, 'little matron'), or nesting dolls. The movement of the nodes is modelled using common equations for the satellite ground track expressed as latitude, ϕ, and longitude, λ. The equations are found in much of the literature regarding constellation design. Arnas & Linares [13] use the expressions to find "loops" in non-intersecting orbital trajectories, Lifson et al [12] use the equations to represent variations in semi-major axis in terms of Latitude, and Ortore et al [18] use these equations to calculate the ground track position of satellites phased by a variation in certain orbital parameters. MatrON uses these equations to describe the satellite position relative to a rotating Earth over time without being bound to a reference epoch attained from Two Line Elements (TLE's) or other observational data. They are also capable of being processed into an "embarrassingly parallel" format i.e. completely independent from one another. This property has been exploited in the field of artificial intelligence by Li et al [19] to train large language models more efficiently and herein can be exploited using parallel computing to calculate large numbers of nodal interactions for multiple shells simultaneously.

Using these equations MatrON consolidates multiple constellations into a single, heterogeneous system of systems which allows pair-wise node interactions to be considered based on the nodes' motion as projected onto a common surface. This paper will describe the development of the MatrON model and the potential it holds. First, a derivation of the Field of Regard (FOR) of any given satellite on the shells below it is given. The expression for the Earth-Centric-Angle (ECA) in terms of Latitude and Longitude is then derived. These expressions then enable the construction of a contact plan.

2. Model Derivation

2.1 Field of Regard

The equations describing the ground track of a satellite are given in Eq. 1 & 2 in their standard form. A full derivation can be found using the vector rotation method in [20], however they can be derived in other ways.

$$\phi_{ss} = \operatorname{asin}(\sin(\mathrm{i})\sin(\mathrm{u}))\,, \tag{1}$$

$$\lambda_{ss} = \operatorname{atan}\left(\frac{\cos(\mathrm{i})\sin(\mathrm{u})}{\cos(\mathrm{u})}\right) + \Omega_0 - \Omega_{\mathrm{Rm}_{\mathrm{t}0}} + \left(\frac{\mathrm{d}\Omega}{\mathrm{dt}} - \frac{\mathrm{d}\Omega_{\mathrm{Rm}}}{\mathrm{dt}}\right)(\mathrm{t} - \mathrm{t}_0)\,, \tag{2}$$

where ϕ_{ss} & λ_{ss} are latitude and longitude respectively, i is the inclination angle of the orbital plane, u is the argument of latitude, Ω_0 represents the initial longitude of the Right Ascension of the Ascending Node (RAAN) and Ω_{Rm} represents the longitude of a reference meridian. The rotational velocity of Ω_{Rm} is simply the rotational rate of the Earth and the rotational velocity of Ω is the rotation of the orbital plane due to any perturbations. The dominant perturbation is that of J_2, caused by Earth's gravitational potential. Its magnitude depends on altitude, inclination and eccentricity of the orbit [21]. These orbital elements can fluctuate over time and so the effect of J_2 is typically not constant at an instantaneous level. This work focusses on circular orbits and so the effects of J_2 can be considered a constant for each individual spacecraft. This circular approximation allows Eq. (1) & (2) to take on the property of being "embarrassingly parallel" as the ground track coordinates at each timestep can be calculated without any dependency on previous timesteps. This property persists through all further derived equations however it is important to note that this property may be lost when improving their accuracy due to the addition of time-dependant perturbations.

Given that Equations (1) & (2) can describe the sub-satellite point of a satellite at any time, t, it is also possible to determine the field of regard of the satellite at this time by considering the satellites cone of regard (COR) intersecting the Earth.

Consider a cone with apex at the satellite ascending node, x_0, along the x-axis extending radially inward towards the Earth. The Earth as assumed to be a perfect sphere of radius R_E centred at the origin. The cartesian equation of the cone is

$$(x - x_0)^2 = \frac{z^2 + y^2}{c^2}\,. \tag{3}$$

Here, c, represents the opening parameter of the cone which is the ratio of the radius of the cone base, r_b, to its height, h,

$$c = {r_b}/{h}\,, \tag{4}$$

and r_b is a function of the cone height and the half-angle of the cone, $\theta_{1/2}$ such that

$$r_b = h \cdot \tan\left(\theta_{1/2}\right). \quad (5)$$

The cartesian equation of the spherical Earth is,

$$x^2 + y^2 + z^2 = R_E^2 . \quad (6)$$

By rearranging Eq. (3) and substituting it into Eq. (6),

$$x^2 + c^2(x - x_0)^2 = R_E^2 , \quad (7)$$

$$(1 + c^2)x^2 + (-2c^2x_0)x + c^2x_0^2 - R_E^2 = 0 . \quad (8)$$

From here the quadratic equation can be used,

$$x = \frac{2c^2x_0 \pm \sqrt{4}\sqrt{c^4x_0^2 - c^2x_0^2 + R_E^2 - c^4x_0^2 + c^2R_E^2}}{2(1+c^2)}, \quad (9)$$

showing that the curve of the intersection is planar with planes located at 2 values of x. Only the first intersection of the cone and sphere is of interest and so by simplifying, this value, x_{int}, can be found,

$$x_{int} = \frac{c^2x_0 + \sqrt{c^2(R_E^2 - x_0^2) + R_E^2}}{1+c^2} . \quad (10)$$

The curve of the intersection is all points on the sphere that also exist on a plane intersecting the sphere at x_{int}.

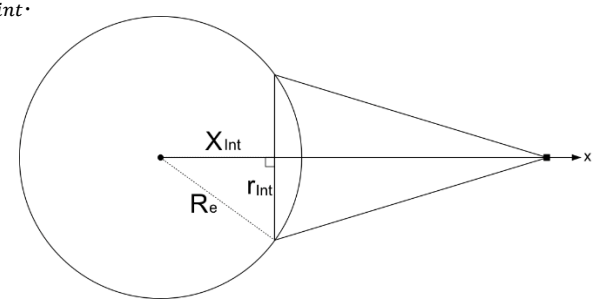

Figure 1: Intersection geometry of COR and Earth

From the geometry in Figure 1, any point on the intersection must lie at a distance R_E from the centre of the Earth but also at a fixed distance r_{int} from the point $[x_{int}, 0, 0]$. The curve is therefore a circle and the radius can be found to be,

$$r_{int} = \sqrt{R_E^2 - x_{int}^2} . \quad (11)$$

The cartesian coordinates of this circle can be expressed as,

$$\begin{bmatrix} x \\ y \\ z \end{bmatrix}_{int} = \begin{bmatrix} x_{int} \\ r_{int}\sin(\theta) \\ r_{int}\cos(\theta) \end{bmatrix}, \quad (12)$$

for $\theta \in (0, 2\pi]$

For a circular orbit, the height of the cone, h, represents the visual range of the satellite and is constant. If it is further assumed that the cone of regard is always pointing radially inwards to the centre of the Earth, the dimensions of the curve of intersection will be constant for any point in the orbit. Therefore, this circle can simply be rotated about the origin according to the latitude and longitude of the sub-satellite point. First by the longitude about the z-axis and then by the latitude about the y-axis. Using a standard right-handed rotation convention, the rotation matrices used are,

$$T_{\lambda_{ss}} = \begin{bmatrix} \cos(\lambda_{ss}) & -\sin(\lambda_{ss}) & 0 \\ \sin(\lambda_{ss}) & \cos(\lambda_{ss}) & 0 \\ 0 & 0 & 1 \end{bmatrix}, \quad (13)$$

$$T_{\phi_{ss}} = \begin{bmatrix} \cos(-\phi_{ss}) & 0 & \sin(-\phi_{ss}) \\ 0 & 1 & 0 \\ -\sin(-\phi_{ss}) & 0 & \cos(-\phi_{ss}) \end{bmatrix}. \quad (14)$$

These are then multiplied together and simplified to provide the full transform,

$$T_{\lambda_{ss}\phi_{ss}} = \begin{bmatrix} \mathrm{c}(\lambda_{ss})\,\mathrm{c}(\phi_{ss}) & -\mathrm{s}(\lambda_{ss}) & -\mathrm{c}(\lambda_{ss})\,\mathrm{s}(\phi_{ss}) \\ \mathrm{s}(\lambda_{ss})\,\mathrm{c}(\phi_{ss}) & \cos(\lambda_{ss}) & -\mathrm{s}(\lambda_{ss})\,\mathrm{s}(\phi_{ss}) \\ \mathrm{s}(\phi_{ss}) & 0 & \mathrm{c}(\phi_{ss}) \end{bmatrix}, \quad (15)$$

where $c = cos$ & $s = sin$.

By using Eq. 15 to rotate the circular intersection the cartesian coordinates of the satellite FOR at any given point in its orbit are acquired,

$$\begin{bmatrix} x \\ y \\ z \end{bmatrix}_{FOR} = \begin{bmatrix} x_{int}\,\mathrm{c}(\lambda_{ss})\,\mathrm{c}(\phi_{ss}) - r_{int}[\mathrm{s}(\theta)\,\mathrm{s}(\lambda_{ss}) + \mathrm{c}(\theta)\,\mathrm{c}(\lambda_{ss})\,\mathrm{s}(\phi_{ss})] \\ x_{int}\,\mathrm{s}(\lambda_{ss})\,\mathrm{c}(\phi_{ss}) + r_{int}[\mathrm{s}(\theta)\,\mathrm{c}(\lambda_{ss}) - \mathrm{c}(\theta)\,\mathrm{s}(\lambda_{ss})\,\mathrm{s}(\phi_{ss})] \\ x_{int}\,\mathrm{s}(\phi_{ss}) + r_{int}\,\mathrm{c}(\theta)\,\mathrm{c}(\phi_{ss}) \end{bmatrix} \quad (16)$$

Using the geometric conversion found in [20]:

$$\begin{bmatrix} x \\ y \\ z \end{bmatrix} = \begin{bmatrix} r \cdot \cos(\phi)\cos(\lambda) \\ r \cdot \cos(\phi)\sin(\lambda) \\ r \cdot \cos(\phi) \end{bmatrix}, \quad (17)$$

these cartesian equations can be represented as latitude and longitude,

$$\phi_{FOR} = \mathrm{asin}\left(\frac{z_{FOR}}{R_E}\right) = \mathrm{asin}\left(\frac{x_{int}\sin(\phi_{ss}) + r_{int}\cos(\theta)\cos(\phi_{ss})}{R_E}\right), \quad (18)$$

$$\lambda_{FOR} = \mathrm{atan}\left(\frac{y_{FOR}}{x_{FOR}}\right) = \mathrm{atan}\left(\frac{x_{int}\,\mathrm{s}(\lambda_{ss})\,\mathrm{c}(\phi_{ss}) + r_{int}[\mathrm{s}(\theta)\,\mathrm{c}(\lambda_{ss}) - \mathrm{c}(\theta)\,\mathrm{s}(\lambda_{ss})\,\mathrm{s}(\phi_{ss})]}{x_{int}\,\mathrm{c}(\lambda_{ss})\,\mathrm{c}(\phi_{ss}) - r_{int}[\mathrm{s}(\theta)\,\mathrm{s}(\lambda_{ss}) + \mathrm{c}(\theta)\,\mathrm{c}(\lambda_{ss})\,\mathrm{s}(\phi_{ss})]}\right). \quad (19)$$

For $\theta \in (0, 2\pi]$, these equations provide latitude and longitude coordinates describing the edge of the satellite FOR based on the position of the sub-satellite point, satellite altitude and cone-of-regard half-angle.

2.2 Earth-Centric Angle

To determine a contact all that must be determined is if a target lies within a satellite FOR on that shell. This is done using the Earth-centric angle (ECA) between the target and the satellite. Take the vectors $\boldsymbol{n}$ & $\boldsymbol{t}$ to be the cartesian positions of a node and a target, respectively. The angle between these two vectors can be found using,

$$\theta = \operatorname{acos}\left(\frac{\boldsymbol{n}\cdot\boldsymbol{t}}{|\boldsymbol{n}||\boldsymbol{t}|}\right). \quad (20)$$

Consider that the node and target exist on a spherical surface such that $|\boldsymbol{n}| = |\boldsymbol{t}| = \boldsymbol{r}$. By expanding Eq. 20 with Eq. 16 and using the trigonometric identity $\cos(\alpha)\cos(\beta) + \sin(\alpha)\sin(\beta) = \cos(\alpha - \beta)$,

$$\theta_{ECA} = \operatorname{acos}(\cos(\phi_n)\cos(\phi_t)\cos(\lambda_n - \lambda_t) + \sin(\phi_n)\sin(\phi_t)). \quad (21)$$

The angle θ_{ECA} is the angle between two points on the surface of a sphere expressed in terms of their respective latitude and longitude. Using this expression, the angular coverage of the satellite FOR can be calculated and used to determine if the target is ever within this coverage during an orbit and for how long. The angular coverage of the FOR, θ_{min}, can be found by choosing any point on the FOR as a target for Eq. 21 and the associated sub-satellite point as the node. Using target location data alongside equations 1, 2 and 21 contact information can be found for an arbitrary number of satellites and targets over any span of time divorced from the constraint of an epoch.

4. Results and Discussion

4.1 Case Study – Sentinel 2

The following section will show a comparison between the MatrON model as described and a simulation of the orbits of the Sentinel 2 constellation using real-world observational data: TLEs available from spacetrack.org [22]. Elements of the Skyfield python library are used to propagate between two successive TLEs using an SGP4 propagation routine [23]. This method is then repeated between each TLE collected over the year 2021 and contacts between the satellites and the latitude and longitude associated to the target city, Bobo-Dioulasso, are collected. The number of contacts is then compared to the number predicted by the MatrON model.

The Sentinel 2 constellation contains only 2 satellites, Sentinel 2A and Sentinel 2B, each in an orbit with a ground track that repeats approximately every 10 days. Each orbit is at an altitude of 786km, inclination of 98.2° and separated in u by 180° [24]. The observational instruments on-board have a field of view of approximately 20.6° [25]. Using this data alongside TLEs the numerical simulation estimates 146 contacts with the target city Bobo-Dioulasso at $\phi = 11°$, $\lambda = 4.3°$. The runtime for this simulation was 33.9 seconds. MatrON predicts 152 contacts, an error of 4%, in 17.9 seconds, a 52.8% improvement. The error can be accounted for in the lack of compensation for orbital perturbations in the ground track equations as well as the assumption that the satellites FOR is circular. Given the accuracy of this initial example for the given runtime improvement, it is clear to see the value that could be gained from using MatrON to assess a large-scale constellation.

4.2 Scaled Example

For 5 orbital shells with 2 satellites in each the altitudes, inclinations and RAAN are given in table 1 in degrees (°). Coordinates are calculated at 30s timesteps and each shell is separated by an altitude of 200km. Each Orbit also begins its propagation at $u = 0°$.

Table 1: Orbital Elements of Test Satellites

Shell number & Altitude	Satellite Number	i(°)	Ω(°)
1: 200km	1	93	271
	2	137	24
2: 400km	1	27	199
	2	11	281
3: 600km	1	156	47
	2	25	169
4: 800km	1	4	301
	2	58	106
5: 1000km	1	112	10
	2	60	37

Targets were chosen arbitrarily; their coordinates are given in table 2.

Table 2: Target Locations

	T1	T2	T3	T4
ϕ_T(°)	45	-9	0	-45
λ_T(°)	45	-9	200	120

For the sake of clarity in presenting the preliminary results, all satellites in all shells have been constrained to the same $\theta_{1/2}$ of 50°. By constraining all satellites in the model to the same COR there will exist a series of

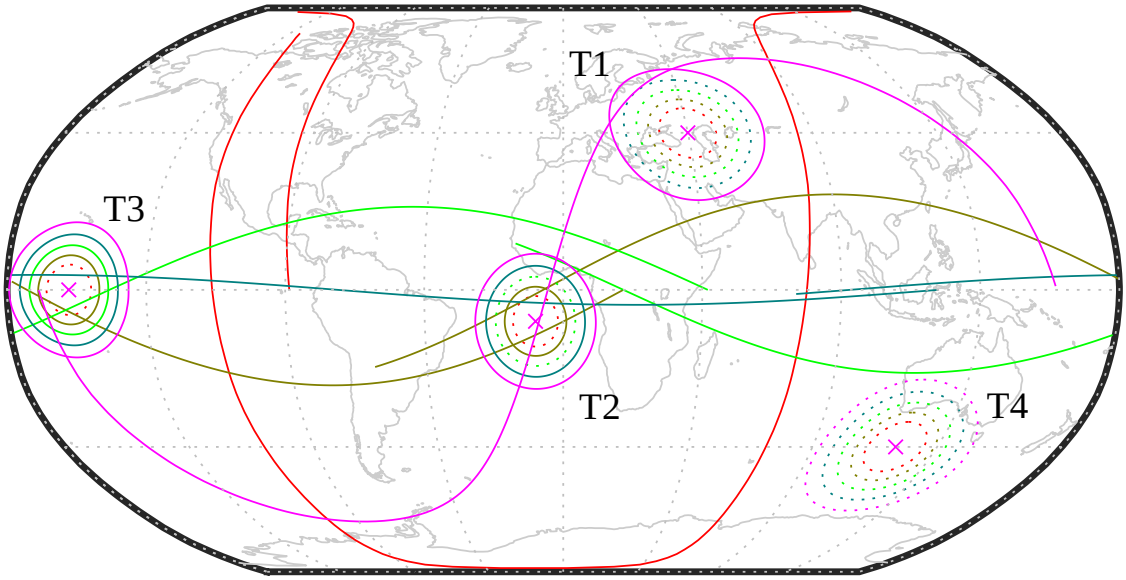

Figure 2: Ground Tracks and CZ's for each shell projected on to Robinson projection of Earth

progressively larger FOR's, associated with each shell altitude. As these FOR's are perfectly circular, they can be layered on top of any arbitrary number of ground targets to show a series of concentric rings around them. These rings represent the contact zone (CZ) within which a satellites ground track indicates the satellite and target are in contact.

Figure 2 shows the ground track / target interactions on a Robinson map projection of the Earth with each colour representing a different shell. Solid circles indicate a CZ that has been intersected by a corresponding ground track. For clarity, only the first ground track for each shell is shown.

The satellite on shell 2 intersects CZ 2 twice and CZ 3 once creating 3 contacts. Shell 3's satellite intersects only the corresponding CZ of target 3 creating just one contact. The satellite on shell 4 intersects targets 2 & 3 once each, making 2 contacts. The ground track for shell 5 can be seen intersecting the corresponding CZs of targets 1,2 & 3 creating 3 contacts and the satellite on shell 1 intersects none of the target CZ's therefore having no contacts. Table 3 shows the contact plan generated for all of these contacts as well as the contacts of the second satellite on each shell.

The results show MatrONs ability to model the interactions of many agents concurrently. This can be used in the analysis of interactions between spacecraft with different concepts of operation, particularly between large-scale satellite constellations operated by different stakeholders. By finding unseen interactions between spacecraft and targets, this can provide insight into how the orbital space is being used and offer improvements to service delivery. As more agents are added to the network, opportunities for interaction/cooperation between constellations will be found and the Earths entire orbital environment will be modelled as one single heterogeneous system of systems.

Table 3: Contact Plan of Preliminary Results

Shell	Satellite	Target	Start	End	Duration
1	2	3	30	90	60
2	1	2	390	690	300
	1	2	6330	6570	240
	1	3	2850	3120	270
	2	3	5280	5400	120
3	1	3	3360	3780	420
	2	2	3480	3960	480
4	1	2	2100	2640	540
	1	3	4800	5340	540
	2	1	4350	4950	600
	2	4	2310	2820	510
5	1	1	4770	5220	450
	1	2	3090	3900	810
	1	3	30	450	420
	2	3	30	510	480
	2	3	6870	7320	450
	2	4	1620	2100	480

5. Conclusions

The MatrON model was able to predict contacts of the Sentinel 2 constellation with a target city much faster than a simulation using SGP4 and TLE data while accruing only a small reduction in accuracy. This was then scaled up to an arbitrarily dense orbital environment containing 10 satellites in 5 orbital shells and 4 ground targets. Due to the simplified nature of the model, a contact plan was generated describing all interactions

between every agent in the network for a low computational cost. This paves the way for analysis of large-scale orbital networks containing many constellations operated by different stakeholders.

Acknowledgements

This material is based upon work supported by the Air Force Office of Scientific Research under award number FA8655-22-1-7010.

References

[1] N. Reiland, A. J. Rosengren, R. Malhotra, and C. Bombardelli, 'Assessing and minimizing collisions in satellite mega-constellations', *Adv. Space Res.*, vol. 67, no. 11, pp. 3755–3774, Jun. 2021, doi: 10.1016/j.asr.2021.01.010.

[2] 'UNOOSA Published Annual Report 2022 | UN-SPIDER Knowledge Portal'. https://www.un-spider.org/news-and-events/news/unoosa-published-annual-report-2022 (accessed Jun. 01, 2023).

[3] 'e-Submission of Satellite Network Filings'. https://www.itu.int/ITU-R/space/asreceived/Publication/DisplayPublication/32322 (accessed Jun. 13, 2023).

[4] W. Zhang, X. Wang, W. Cui, Z. Zhao, and S. Chen, 'Self-induced collision risk of the Starlink constellation based on long-term orbital evolution analysis', *Astrodynamics*, Aug. 2023, doi: 10.1007/s42064-023-0171-7.

[5] G. A. Badikov and A. V. Zaytsev, 'Economic model of costs required to create and operate the Starlink fast internet system', presented at the XLV ACADEMIC SPACE CONFERENCE, DEDICATED TO THE MEMORY OF ACADEMICIAN S.P. KOROLEV AND OTHER OUTSTANDING NATIONAL SCIENTISTS — PIONEERS OF SPACE EXPLORATION, Moscow, Russia, 2023, p. 200002. doi: 10.1063/5.0107984.

[6] G. Kay, 'Everything we know about Elon Musk's Starlink satellites and future internet plans', *Business Insider*. https://www.businessinsider.com/elon-musk-starlink-satellites-internet (accessed Aug. 16, 2023).

[7] J. A. Hu, M. L. Rawls, P. Yoachim, and Ž. Ivezić, 'Satellite Constellation Avoidance with the Rubin Observatory Legacy Survey of Space and Time', *Astrophys. J. Lett.*, vol. 941, no. 1, p. L15, Dec. 2022, doi: 10.3847/2041-8213/aca592.

[8] D. J. Kessler and B. G. Cour-Palais, 'Collision frequency of artificial satellites: The creation of a debris belt', *J. Geophys. Res. Space Phys.*, vol. 83, no. A6, pp. 2637–2646, 1978, doi: 10.1029/JA083iA06p02637.

[9] United Nations Office for Outer Space Affairs, *Guidelines for the Long-term Sustainability of Outer Space Activities of the Committee on the Peaceful Uses of Outer Space*. United Nations, 2022. doi: 10.18356/9789210021852.

[10] 'ESA's Space Environment Report 2022'. https://www.esa.int/Space_Safety/Space_Debris/ESA_s_Space_Environment_Report_2022 (accessed Aug. 23, 2023).

[11] T. J. Colvin, J. Karcz, G. Wusk, P. Besha, and B. Naasz, 'Cost and Benefit Analysis of Orbital Debris Remediation'.

[12] M. Lifson, D. Arnas, M. Avendaño, and R. Linares, 'A Method for Generating Closely Packed Orbital Shells and the Implication on Orbital Capacity'. arXiv, Mar. 24, 2022. doi: 10.48550/arXiv.2203.13354.

[13] D. Arnas and R. Linares, 'Non-Self-Intersecting Trajectories and Their Applications to Satellite Constellation Design and Orbital Capacity', *J. Guid. Control Dyn.*, vol. 46, no. 3, pp. 417–430, 2023, doi: 10.2514/1.G007208.

[14] M. Lifson, A. D'Ambrosio, D. Arnas, and R. Linares, *HOW MANY SATELLITES CAN WE FIT IN LOW EARTH ORBIT?: CAPACITY INTEGRATING RISK-BASED AND INTRINSIC METHODS*. 2022.

[15] D. Ly, R. Lucken, and D. Giolito, 'Correcting TLEs at epoch: Application to the GPS constellation', *J. Space Saf. Eng.*, vol. 7, no. 3, pp. 302–306, Sep. 2020, doi: 10.1016/j.jsse.2020.07.032.

[16] D. Conkey and M. Zielinski, 'Assessing Performance Characteristics of the SGP4-XP Propagation Algorithm', 2022.

[17] A. Holincheck and J. Cathell, 'Improved Orbital Predictions using Pseudo Observations - Maximizing the Utility of', 2021.

[18] E. Ortore, M. Cinelli, and C. Circi, 'A ground track-based approach to design satellite constellations', *Aerosp. Sci. Technol.*, vol. 69, pp. 458–464, Oct. 2017, doi: 10.1016/j.ast.2017.07.006.

[19] M. Li *et al.*, 'Branch-Train-Merge: Embarrassingly Parallel Training of Expert Language Models'. arXiv, Aug. 05, 2022. Accessed: Jun. 26, 2023. [Online]. Available: http://arxiv.org/abs/2208.03306

[20] M. Capderou, 'Ground Track of a Satellite', in *Handbook of Satellite Orbits: From Kepler to GPS*, M. Capderou, Ed., Cham: Springer International Publishing, 2014, pp. 301–338. doi: 10.1007/978-3-319-03416-4_8.

[21] H. D. Curtis, *Orbital Mechanics for Engineering Students: Revised Reprint*. Butterworth-Heinemann, 2020.

[22] 'Space-Track.org'. https://www.space-track.org/auth/login (accessed Aug. 31, 2023).

[23] B. Rhodes, 'Skyfield: High precision research-grade positions for planets and Earth satellites generator', *Astrophys. Source Code Libr.*, p. ascl:1907.024, Jul. 2019.

[24] 'Orbit - Sentinel 2 - Mission - Sentinel Online', *Sentinel Online*. https://copernicus.eu/missions/sentinel-2/satellite-description/orbit (accessed Aug. 31, 2023).

[25] D. P. Roy, J. Li, H. K. Zhang, L. Yan, H. Huang, and Z. Li, 'Examination of Sentinel-2A multi-spectral instrument (MSI) reflectance anisotropy and the suitability of a general method to normalize MSI reflectance to nadir BRDF adjusted reflectance', *Remote Sens. Environ.*, vol. 199, pp. 25–38, Sep. 2017, doi: 10.1016/j.rse.2017.06.019.